First-principles investigation on chemical bonding and bulk modulus of the ternary carbide $Zr_2Al_3C_5$

Jingyang Wang,[1,2] Yanchun Zhou,[1] Zhijun Lin,[1] and Ting Liao[1]
[1]*Shenyang National Laboratory for Materials Science, Institute of Metal Research, Chinese Academy of Sciences, Shenyang, 110016, China*
[2]*International Centre for Materials Physics, Institute of Metal Research, Chinese Academy of Sciences, Shenyang 110016, China*
(Received 18 January 2005; published 1 August 2005)

We have investigated the electronic structure, chemical bonding, and equations of state of $Zr_2Al_3C_5$ by means of the *ab initio* pseudopotential total energy method. The chemical bonding displays layered characteristics and is similar to that of nanolaminate ternary aluminum carbides Ti_2AlC and Ti_3AlC_2. $Zr_2Al_3C_5$ could be fundamentally described as strong covalent bonding among Al-C-Zr-C-Zr-C-Al atomic chains being interleaved and mirrored by AlC_2 blocks. The interplanar cohesion between covalent atomic chains and AlC_2 blocks is very weak based on first-principles cohesion energy calculations. Inspired by the structure-property relationship of Ti_2AlC and Ti_3AlC_2, it is expected that $Zr_2Al_3C_5$ will have easy machinability, damage tolerance, and oxidation resistance besides the merits of refractory ZrC. $Zr_2Al_3C_5$ has a theoretical bulk modulus of 160 GPa and illustrates elastic anisotropy under pressure below 20 GPa.

DOI: 10.1103/PhysRevB.72.052102 PACS number(s): 81.05.Je, 71.20.−b, 62.20.Dc

Zirconium carbide (ZrC) is a refractory transition metal carbide (TMC) which is characterized by high hardness, high strength, high melting point, good thermal shock and wear resistance, chemical inertness, and absence of phase changes in the solid state. These properties give ZrC the potential to be used in ultrahigh temperature environments. Barriers to its more extensive applications are the poor oxidation resistance and intrinsic low toughness. An important way to overcome the difficulty is to incorporate Al to form ternary compound.

Schuster *et al.* have identified some machinable ternary TMCs, i.e., *MAX* phases such as Ti_2AlC and Nb_2AlC.[1] Two fundamental structural blocks are in the *MAX* phase, the nonstoichiometric TMC unit and planar packed Al layers. The crystal structure of ternary TMC can be described as the nanoscale sheets of nonstoichiometric binary edge-shared TMC octahedra being intercalated by close-packed Al atomic planes. The ternary *MAX* phases exhibit astonishing properties, such as easy machinability, high-temperature oxidation resistance, damage tolerance, and microscale ductility at room temperature due to their nanolaminated crystal structure.[2] In addition, most of the ternary *MAX* phases conserve the common mechanical and electrical properties of their binary TMC counterparts.

Unlike in ternary Ti-Al-C and Nb-Al-C systems, no compound with the structure of *MAX* phases has been identified in the Zr-Al-C system.[1] The equilibrium phase diagram of the ternary Zr-Al-C system includes three ternary compounds, $Zr_2Al_3C_5$, $Zr_3Al_3C_5$ (previously reported with the formula $ZrAlC_{2-x}$ in Ref. 3), and Zr_5Al_3C. Although having been identified for a long time, these ternary Zr-Al-C compounds are limitedly investigated. The reasons are attributed to the difficulties in synthesizing bulk materials and lack of theoretical predictions on mechanical and chemical properties. $Zr_2Al_3C_5$ belongs to the $P6_3/mmc$ space group[4] and its crystal structure is shown in Fig. 1. The Al and C atoms are indexed with various numbers according to different coordination environments. The crystal structure of $Zr_2Al_3C_5$ illustrates similar characteristics to those of the *MAX* phases. For example, the nonstoichiometric ZrC_x blocks exist in $Zr_2Al_3C_5$; and, in addition, planar close-packed Al and C atoms interleave these ZrC_x blocks. It is, therefore, likely that $Zr_2Al_3C_5$ will exhibit well-designed properties.

Our aim is to investigate the characteristics of chemical bonds in $Zr_2Al_3C_5$ and to study if the compound illustrates layered characteristics in the electronic scale. If weak interplanar bonding exists in $Zr_2Al_3C_5$, the material is expected to have similar mechanical properties to the *MAX* phases. In other words, $Zr_2Al_3C_5$ will be machinable, damage tolerant,

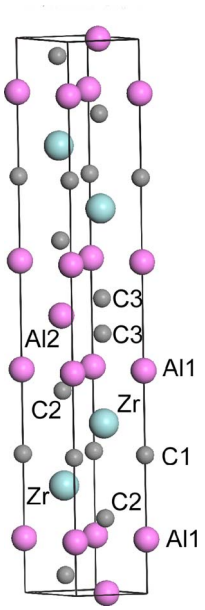

FIG. 1. (Color online) Crystal structure of $Zr_2Al_3C_5$. The Al and C atoms are labeled with numbers according to various coordination environments.

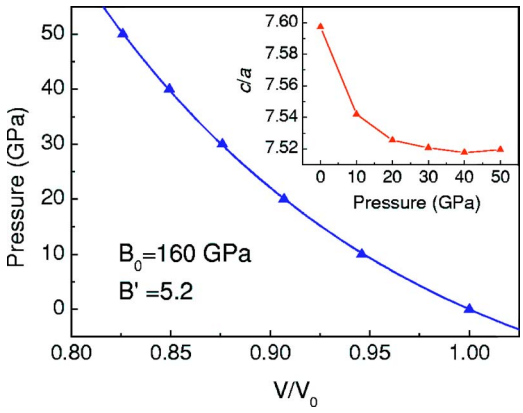

FIG. 2. (Color online) Relative unit cell volume V/V_0 as a function of external pressure. The inset shows the axial ratio c/a varying with pressure.

and oxidation resistant. Unfortunately, only the crystallography information of $Zr_2Al_3C_5$ has been reported until now. With these anticipating properties, we focus on the electronic band structure, chemical bonding characteristics, equations of state (EOS), and bulk modulus of $Zr_2Al_3C_5$ with the help of first-principles calculations. Our results indicate that $Zr_2Al_3C_5$ will exhibit similar salient properties to the *MAX* phases. Furthermore, we provide predictive clues on overcoming the difficulties that encumber the applications of ZrC.

Using the CASTEP code in the present calculations,[5] the Vanderbilt-type ultrasoft pseudopotential[6] and generalized gradient approximation[7] (GGA-PW91) were employed. The plane-wave basis set cutoff was 450 eV for all calculations. The special points sampling integration over the Brillouin zone was employed by using the Monkhorst–Pack method with a $10\times10\times2$ special k-points mesh.[8] To investigate the ground state electronic band structure and EOS, the lattice configurations were obtained at various isotropic hydrostatic pressures ranging from 0 to 50 GPa. Lattice parameters, including lattice constants and internal atomic coordinates, were modified independently to minimize the free enthalpy, interatomic forces and unit-cell stresses. The Brodyden–Fletcher–Goldfarb–Shanno (BFGS) minimization scheme[9] was used in geometry optimization. The tolerances for geometry optimization were: difference on total energy within 5×10^{-6} eV/atom, maximum ionic Hellmann–Feynman force within 0.01 eV/Å, maximum ionic displacement within 5×10^{-4} Å and maximum stress within 0.02 GPa. The present first-principles calculation scheme is reliable on predicting equilibrium crystal structure and elastic stiffness for ternary transition metal carbides.[10,11]

Figure 2 shows the relative unit cell volume V/V_0 as a function of external pressure. Our theoretical equilibrium volume, 217.68 Å^3, is within 2% deviation of the experimental volume.[1] By fitting the data with the Birch–Murnaghan equation,[12] bulk modulus B_0 and its pressure derivative B_0' are obtained to be 160 GPa and 5.2, respectively. The bulk modulus of $Zr_2Al_3C_5$ is about 70% of that of ZrC, which is 229 GPa computed within the same first-principles scheme. The inset of Fig. 2 shows the axial ratio c/a varying with pressure. The c/a decreases rapidly as the pressure increases from 0 to 20 GPa and saturates to a constant value 7.52 with increased pressure. Trend in c/a demonstrates that c contracts more rapidly than a below 20 GPa. The elastic stiffness along c is lower than that along basal plane when $Zr_2Al_3C_5$ is imposed under pressure. Therefore, $Zr_2Al_3C_5$ is anisotropic in elastic stiffness when external pressure is relatively small. The elastic anisotropy indicates that the intraplanar atomic bonds are stronger than the interplane bonds. When the contractions of a and c exceed a critical value (c/a less than 7.52), the material becomes elastic isotropy. Similar trends have been found in the *MAX* phases, such as anisotropic elastic stiffness of Ti_3SiC_2 under pressure.[13]

To identify the characteristics of chemical bonds, the electronic structure is analyzed. The calculations of partial density of states (PDOS) were performed using a projection of the plane-wave electronic states onto a localized linear combination of atomic orbitals (LCAO) basis set. In the present calculation, the LCAO basis set was the atomic pseudo-orbitals corresponding to the close valence shell containing the valence electrons. According to these, the numbers of pseudo-orbitals were chosen as 4 for C, 3 for Al, and 9 for Zr, respectively. Then the s, p valence orbitals of C were included in calculation of PDOS, as well as s, p orbitals of Al or s, p, and d orbitals of Zr, respectively. Since $Zr_2Al_3C_5$ is a metallic system, partial occupancies were introduced to eliminate discontinuous changes in total energy that were created when an energy band crossed a Fermi level during the self-consistant electronic minimization. Twelve additional empty bands were included in the electronic minimization, and we used the Gaussian smearing scheme with a smearing width of 0.1 eV.

In Fig. 3, we show the PDOS of $Zr_2Al_3C_5$. The lowest lying states around −15.4, −10.4, and −9.3 eV originate from the C 2s orbitals. Overlapping of Al1 and C2 orbitals extend from −12.6 to −9.6 eV. The sp-derived and pp-derived hybridization states of Al and C spread from −9.4 eV to the Fermi level. The Zr 4d-C 2p covalent bonding states locate around −2.7 and −2.2 eV, respectively. The higher energy range of Zr-C2 pd hybridization indicates that Zr-C2 is relatively weaker than the Zr-C1 covalent bond. It should be noted that the C3 2p orbitals dominate the states at the Fermi level, with slight contribution from A12 3p and Zr 4d states. The metallic conductivity mainly originates from the π-like p-p derived hybridization of planar packed C3 (0001) atomic planes.

The charge density contour is shown in Fig. 4 for a slice of $(11\bar{2}0)$ plane. Figure 4 shows obvious covalent nature among Al-C-Zr-C-Zr-C-Al atomic chains (abbreviated as $Zr_2Al_2C_3\otimes$). The AlC_2 unit is a strong covalent bonding block that interleaves the $Zr_2Al_2C_3\otimes$ covalent atomic chains. Adjacent $Zr_2Al_2C_3\otimes$ blocks mirror each other according to the AlC_2 unit. The interplanar electronic density is very low in the region connecting $Zr_2Al_2C_3\otimes$ and AlC_2 blocks, which suggests that the interplanar chemical bonding is relatively weak. Investigations on layered *MAX* phases Ti_2AlC and Ti_3AlC_2 showed similar chemical bonding characteristics.[11,14]

In order to evaluate the weak interplanar covalent bonding

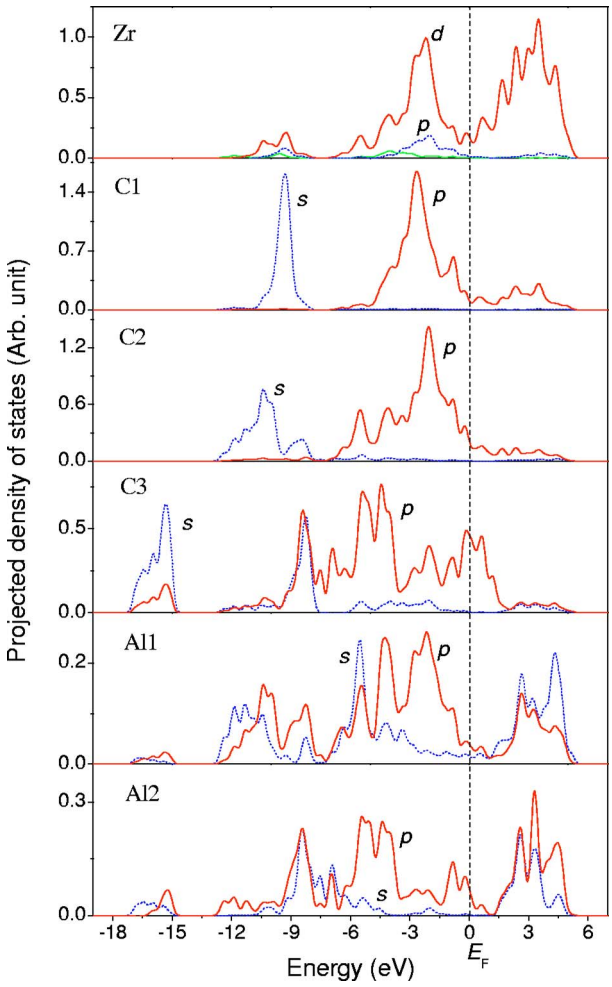

FIG. 3. (Color online) Site and angular momentum projection of electronic density of states of $Zr_2Al_3C_5$.

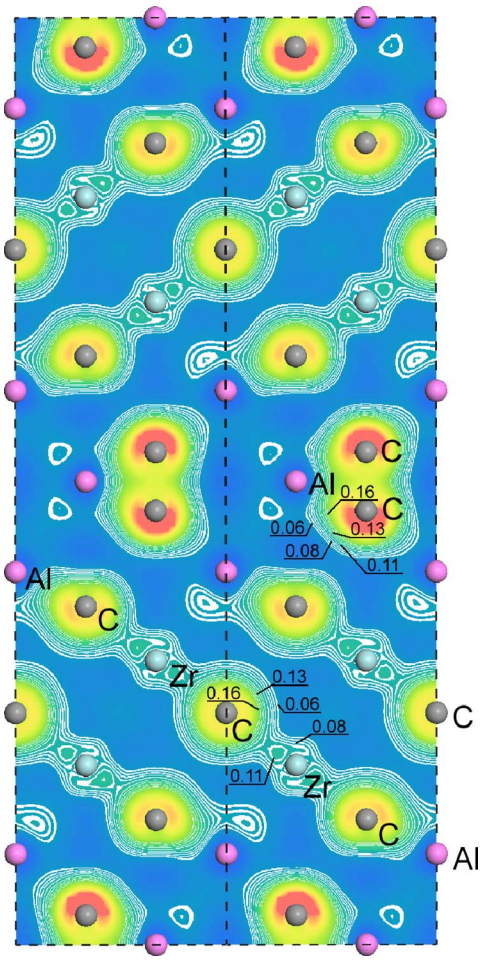

FIG. 4. (Color online) Valence electron density for a slice of $(11\bar{2}0)$ plane. The white contour lines range from 0.06 to 0.16 electrons/Å^3.

between $Zr_2Al_2C_3\otimes$ and AlC_2 blocks (denoted as $\otimes AlC_2$) quantitatively, we calculate the cohesive energy between these blocks. The cut plane cleaves Al1-C3 bonds and is parallel to the basal plane. The cohesive energy E_{coh} is computed by

$$E_{coh} = E_{total}^{Zr_2Al_2C_3\otimes} + E_{total}^{\otimes AlC_2} - E_{total}^{Zr_2Al_3C_5} \quad (1)$$

where the $E_{total}^{Zr_2Al_2C_3\otimes}$ is the total energy of $Zr_2Al_2C_3\otimes$ blocks after eliminating the AlC_2 blocks from the unit cell, $E_{total}^{\otimes AlC_2}$ is the total energy of AlC_2 blocks after eliminating the $Zr_2Al_2C_3\otimes$ blocks from the unit cell, and $E_{total}^{Zr_2Al_3C_5}$ is the total energy of $Zr_2Al_3C_5$. The computed cohesive energy yields 0.35 eV/atom for $Zr_2Al_3C_5$. For comparison, we calculate the cohesive energy between nonstoichiometric TiC_x block and Al atomic plane for Ti_2AlC and Ti_3AlC_2. The cohesive energies are 0.87 and 0.57 eV/atom for Ti_2AlC and Ti_3AlC_2, respectively. The cohesive energy for inter-planar weak bonding in $Zr_2Al_3C_5$ is comparable to (and even smaller than) those in Ti_2AlC and Ti_3AlC_2. The small cohesive energy suggests that the interplanar cohesion between $Zr_2Al_2C_3\otimes$ and AlC_2 blocks is very weak in $Zr_2Al_3C_5$.

We have known that the easy machinability and damage tolerance of Ti_2AlC and Ti_3AlC_2 originate from the weak interplanar cohesion between transition metal carbide blocks and Al atomic planes. In addition, because of weak cohesion of Al atomic planes in the compound, protective Al_2O_3 scale forms in high temperature environments. As a result, the ternary carbides Ti_2AlC and Ti_3AlC_2 demonstrate excellent high-temperature oxidation resistance.[15] For $Zr_2Al_3C_5$, the AlC_2 block is weakly bonded to the $Zr_2Al_2C_3\otimes$ units. Through the weak interplanar chemical bonding, the material can access deformation processes by basal plane slip, cleavage, and delamination; and, therefore, illustrate microscale plasticity, as well as easy machinability. In consequence, $Zr_2Al_3C_5$ is predicted to hold mechanical properties such as damage tolerance and machinability. Furthermore, the cohesive energy between AlC_2 and $Zr_2Al_2C_3\otimes$ blocks is very small, and the AlC_2 unit is highly chemical-active because free electron states dominantly originate from the AlC_2 blocks. Therefore, $Zr_2Al_3C_5$ will illustrate excellent oxidation resistance similar to Ti_2AlC and Ti_3AlC_2.

In summary, we investigated the electronic structure, bonding characteristics, and EOS of $Zr_2Al_3C_5$ by first-principles calculations. Our computed bulk modulus of $Zr_2Al_3C_5$ yields 160 GPa and the material shows elastic anisotropy under pressure below 20 GPa. The chemical bond-

ing displays layered characteristics similar to those of *MAX* phases Ti_2AlC and Ti_3AlC_2. We predict that $Zr_2Al_3C_5$ will exhibit well-designed properties. Therefore, more experimental and theoretical works should be done on $Zr_2Al_3C_5$.

This work was supported by the National Outstanding Young Scientist Foundation for Y.C.Z. under Grant No. 59925208, Natural Sciences Foundation of China under Grant Nos. 50232040, 90403027, and 50302011.

[1] J. C. Schuster and H. Nowotny, Z. Metallkd. **71**, 341 (1980).
[2] M. W. Barsoum, Prog. Solid State Chem. **28**, 201 (2000).
[3] S. I. Mikhalenko, Y. B. Kuz'ma, V. E. Popov, V. N. Gurin, and A. P. Nechitailov, Izv. Akad. Nauk SSSR, Neorg. Mater. **15**, 1948 (1979).
[4] E. Parthe and B. Chabot, Acta Crystallogr., Sect. C: Cryst. Struct. Commun. **C44**, 774 (1988).
[5] M. D. Segall, P. L. D. Lindan, M. J. Probert, C. J. Pickard, P. J. Hasnip, S. J. Clark, and M. C. Payne, J. Phys.: Condens. Matter **14**, 2717 (2002).
[6] D. Vanderbilt, Phys. Rev. B **41**, 7892 (1990).
[7] J. P. Perdew, J. A. Chevary, S. H. Vosko, K. A. Jackson, M. R. Pederson, D. J. Singh, and C. Fiolhais, Phys. Rev. B **46**, 6671 (1992).
[8] H. J. Monkhorst and J. D. Pack, Phys. Rev. B **16**, 1748 (1977).
[9] B. G. Pfrommer, M. Côté, S. G. Louie, and M. L. Cohen, J. Comp. Physiol. **131**, 233 (1997).
[10] J. Y. Wang and Y. C. Zhou, Phys. Rev. B **69**, 144108 (2004).
[11] J. Y. Wang and Y. C. Zhou, Phys. Rev. B **69**, 214111 (2004).
[12] F. Birch, J. Geophys. Res. **83**, 1257 (1978).
[13] A. Onondera, H. Hirano, T. Yuasa, N. F. Gao, and Y. Miyamoto, Appl. Phys. Lett. **74**, 3782 (2004).
[14] Y. C. Zhou, X. H. Wang, Z. M. Sun, and S. Q. Chen, J. Mater. Chem. **11**, 2335 (2001).
[15] X. H. Wang and Y. C. Zhou, Corros. Sci. **45**, 891 (2003).